



# Structure-Specific Nuclease Activities of *Pyrococcus abyssi* RNase HII

Sébastien Le Laz, Audrey Le Goaziou, Ghislaine Henneke

## ► To cite this version:

Sébastien Le Laz, Audrey Le Goaziou, Ghislaine Henneke. Structure-Specific Nuclease Activities of *Pyrococcus abyssi* RNase HII. *Journal of Bacteriology*, 2010, 192 (14), pp.3689-3698. 10.1128/JB.00268-10 . hal-00616999

**HAL Id: hal-00616999**

**<https://hal.univ-brest.fr/hal-00616999>**

Submitted on 2 Sep 2011

**HAL** is a multi-disciplinary open access archive for the deposit and dissemination of scientific research documents, whether they are published or not. The documents may come from teaching and research institutions in France or abroad, or from public or private research centers.

L'archive ouverte pluridisciplinaire **HAL**, est destinée au dépôt et à la diffusion de documents scientifiques de niveau recherche, publiés ou non, émanant des établissements d'enseignement et de recherche français ou étrangers, des laboratoires publics ou privés.

1 **Structure-specific nuclease activities in *Pyrococcus abyssi* RNase HII**

2  
3 Sébastien Le Laz<sup>1</sup>, Audrey Le Goaziou<sup>1, 2</sup> and Ghislaine Henneke<sup>1, 2\*</sup>

4  
5 <sup>1</sup> Université de Bretagne Occidentale, UMR 6197, Laboratoire de Microbiologie des  
6 Environnements Extrêmes, 29280 Plouzané, France.

7 <sup>2</sup> Ifremer, UMR 6197, Laboratoire de Microbiologie des Environnements Extrêmes, BP 70,  
8 29280 Plouzané, France.

9  
10  
11 Running Title: Substrate structure requirements of *Pab*RNase HII

12  
13  
14 \*Corresponding author: Ghislaine HENNEKE, Ifremer, DEEP/LMEE, B.P. 70, 29280  
15 Plouzané, France; Tel.: +33 2 98 22 46 09; Fax: +33 2 98 22 47 57

16 E-mail: [ghenneke@ifremer.fr](mailto:ghenneke@ifremer.fr)

## ABSTRACT

Faithful DNA replication involves the removal of RNA residues from genomic DNA prior to ligation of nascent DNA fragments in all living organisms. Because the physiological roles of archaeal type 2 RNase H are not fully understood, substrate structure requirements for detection of RNase H activity need further clarification. Biochemical characterisation of a single RNase H detected within the genome of *Pyrococcus abyssi* showed that this type 2 RNase H is a Mg<sup>2+</sup>- and alkaline- dependent enzyme. *Pab*RNase HII showed ribonuclease activity and acted as a specific endonuclease on RNA-DNA/DNAs. This specific cleavage, one nucleotide upstream of the RNA-DNA junction, occurred on a substrate in which RNA initiators had to be fully annealed to the complementary DNA template. On the other hand, a 5'-RNA flap Okazaki fragment intermediates impaired *Pab*RNase HII endonuclease activity. Furthermore, introduction of mismatches in the RNA portion near the RNA-DNA junction decreased both specificity and efficiency of cleavage by *Pab*RNase HII. Additionally, *Pab*RNase HII could cleave a single ribonucleotide embedded in a double-stranded DNA. Our data revealed *Pab*RNase HII as a dual-function enzyme likely required for completion of DNA replication and DNA repair.

## INTRODUCTION

DNA replication in all living organisms takes place concurrently on two separate strands. The lagging strand consists of multiple discontinuous segments called Okazaki fragments, whereas the leading strand comprises one large continuous segment. Production of each individual lagging strand by DNA polymerase is primed by a short stretch of RNA. Later on, these RNA primers are eliminated and the resulting gap is filled with deoxyribonucleotides prior to ligation. Priming and DNA elongation at the replication fork involve a set of specialized polymerising enzymes which differ from replicative DNA polymerases, and one another, to correct erroneously inserted nucleotides. In archaeal cells, the priming complex lacks proofreading 3'-5' exonuclease activity (13, 14) present in the replicative DNA polymerases B and D (1, 8). Consequently, mismatches in the vicinity of the RNA-DNA junction could arise in replicating cells, as already observed in eukaryotes (28, 31). Similarly, single ribonucleotides incorporated during DNA replication (20, 26) or by external agents (32) would represent another source of erroneous nucleotides. Persistence of residual RNA during DNA replication would be detrimental for the cells, suggesting that a combination of specific and efficient nucleolytic processes is absolutely required to preserve DNA integrity. Ribonucleases H (RNase H) are enzymes which degrade the RNA portion of RNA/DNA or RNA-DNA/DNA duplexes (29). RNases H are classified into two major families, type 1 and type 2, based on amino acid sequence (21). The type 1 family includes bacterial RNase HI, mammalian RNase HII, the RNase H domain of reverse transcriptase and archaeal RNase HI and the type 2 contains bacterial RNase HII and RNase HIII, mammalian RNase HI and archaeal RNase HII (21). While type 2 RNase H enzymes are universally conserved in the three domains of life, their physiological role remains elusive. Much less is known about the type 2 family compared to the type 1 RNase H enzymes. The multiplicity of RNases H within

a single cell complicates the situation, although presumable roles in DNA replication, DNA repair and transcription have been assigned as recently reviewed (2, 30). In archaea, structural and biochemical characterization of type 2 RNases H (3, 4, 10, 12, 16, 19) suggested they can initiate RNA removal from DNA duplexes, based on their ability to specifically cleave 5' to the junctional ribonucleotide. However, despite this information, the physiological role of type 2 RNases H still remains elusive. They could be involved in the completion of either leading or lagging strands or both. Additional biochemical experiments with catalytic intermediates should provide valuable knowledge on the participation of these archaeal cellular enzymes at the replication fork and in DNA repair.

To investigate this question, we have designed a set of RNA/DNA duplex, cognate RNA-DNA/DNA duplex (15), a single ribonucleotide embedded in a DNA duplex (DNA-1RNA-DNA/DNA) as substrates, and employed type 2 RNase H from the hyperthermophilic deep-sea euryarchaeon *Pyrococcus abyssi* (*Pab*), *PabRNase HII*. Since a single *rnh* gene exists in the genome of *P. abyssi* (6), RNase HII is likely the key enzyme involved in RNA elimination in this organism. Thus, *PabRNase HII* can be considered as the representative of type 2 RNase H.

Here, we analysed the cleavage specificity of *PabRNase HII* for substrates with Okazaki fragment-like structure. We also tested *PabRNase HII* activity on Okazaki fragment-like substrates in the presence of mismatched base pair in order to assess the molecular mechanism of recognition of the RNA-DNA junction and the subsequent cleavage specificity. In addition, we examined whether *PabRNase HII* can incise the DNA backbone on the 5'-side of a single ribonucleotide embedded in a DNA duplex. Our data provide substantial evidences that the single RNase H in *P. abyssi* has a dual role in maintenance of genome integrity. The results from this study are further discussed to define potent roles of type 2 RNase H from *P.*

90 *abyssi* in the resolution of RNA fragments at the replication fork and in the repair of single  
91 embedded ribonucleotides.

## MATERIALS AND METHODS

### Nucleic acid substrates.

Gel-purified oligonucleotides for preparing the substrates for RNase HII assays were purchased from Eurogentec (Belgium) and their sequences are listed in Table 1. Fluorescent labelling at the 5'- end was performed with the 5' End Tag kit labelling system from Vector Laboratories (California). Free fluorescent dyes were removed on MicroSpin™ G-25 columns. For some experiments, 5'-end- or 3'-end-fluorescent labelled oligonucleotides were chemically synthesized and HPLC-purified by Eurogentec (Belgium). To generate the substrates for the RNase HII assays, the appropriate oligonucleotides were mixed in 1:1 molar ratio in 20 mM Tris-HCl (pH 7.4), 150 mM NaCl, heated to 75°C and slowly cooled to room temperature.

### Cloning, production and purification of *Pab*RNase HII.

The gene encoding *Pab*RNase HII (PAB0352) was cloned into the pQE-80L expression vector (Qiagen). *Pab*RNase HII was overexpressed in *E. coli* strain BL21-CodonPlus-RIL strain (Stratagene) as a histidine-tagged protein and purified to near homogeneity via Ni-NTA beads (Qiagen) and S200 gel filtration using fast protein liquid chromatography (GE Healthcare) as previously described (16). Protein integrity was analyzed by MALDI-TOF analyses (Innova Proteomics, France). *Pab*RNase HII purity was controlled by SDS-PAGE gradient gel (4-20 %) electrophoresis (Thermo Scientific).

### Amino acid sequence alignments and secondary structure.

Amino acid sequence alignments have been constructed by ClustalW2 (available at [www.ebi.ac.uk/clustalW2/](http://www.ebi.ac.uk/clustalW2/)). Secondary structure elements calculated with the program

ESPrpt 2.2 (available at <http://esprpt.ibcp.fr/ESPrpt/ESPrpt/>) refer to the structure of *TkoKOD1RNase HII* (PDB: 1IO2).

#### **Assays for RNase HII activity.**

Assays to monitor cleavage by *PabRNase HII* were performed in RNase HII buffer (10 µl) containing: 50 mM Tris-HCl (pH 8), 5 mM dithiothreitol, 5 mM MgCl<sub>2</sub> and 50 nM of DNA substrates. Enzymes were diluted from concentrated stocks in 20 mM Tris-HCl (pH 7.5), 20 % glycerol prior to usage. Enzyme concentrations for a typical reaction ranged from 4 to 400 nM, unless otherwise specified. After addition of *PabRNase HII*, reactions were incubated at 60°C for 30 minutes and stopped on ice with 15 µl of stop buffer (98 % formamide, 10 mM EDTA). Samples were heated at 95°C for 5 minutes. A base hydrolysis ladder was prepared by incubation of the labelled RNA-DNA strand (10 µM) with snake venom phosphodiesterase I (0.018 units) for 10 minutes at 37°C. Product analysis was carried out by electrophoresis on 15 % denaturing polyacrylamide gels. After visualisation with a Mode Imager Typhoon 9400 (GE Healthcare), quantification of the results was performed using ImageQuant 5.2 software. In all cases, the percentage of substrate hydrolysis was determined by the products / (products + substrate) ratio, allowing a correction for loading errors and a comparison of cleavage efficiency irrespective of the different products generated.

To analyse divalent cations or pH dependence, RNase HII assays were carried out with 50 nM of *PabRNase HII* and 50 nM of the S1 substrate at 60°C for 30 min. Data are the average of triplicate measurements and are shown with standard deviations (SD).

To determine the kinetic parameters, steady-state kinetic reactions were carried out in the same conditions as described above by using substrate 1 at concentrations ranging from 0.03 to 3 µM. Initial velocity experiments were monitored as a function of time with 60 nM of *PabRNase HII* at 60°C such that the rate of converted substrate did not exceed 20 % of the



142 total. Velocity measurements were reported as the amount of hydrolysed substrate ( $\mu\text{M}$ ) over  
143 time (min). The observed rates of converted substrates with *PabRNase HII* were firstly  
144 determined from Lineweaver-Burk plots. The data were fit by nonlinear regression using the  
145 Marquardt-Levenberg algorithm (EnzFitter 2.0, BioSoft) to the Michaelis-Menten equation.  
146 Kinetic parameters,  $K_m$  and  $V_{\text{max}}$ , were obtained from the fit and were used to calculate the  
147 catalytic efficiency ( $k_{\text{cat}}/K_m$ ) of *PabRNase HII*. The kinetics values are the average of at least  
148 triplicate determinations and are shown with standard deviations (SD). Any adjustments to the  
149 above are noted in the Figure Legends.

## RESULTS

### Archaeal RNase HII homologues

*Pab*RNase HII showed amino acid sequence similarities of 75.2 % with *Tko*RNase HII, and 65 % with *Afu*RNase HII. Analysis of protein primary structures and related secondary structures outlined subtle differences between the three proteins (Fig. 1A). On the one hand, *Pab*RNase HII and *Afu*RNase HII are isoelectric at basic pH (isoelectric point values of 9 and 7.6, respectively), whereas *Tko*RNase HII is isoelectric at acidic pH (isoelectric point of 5.5). On the other hand, *Pab*RNase HII, *Tko*RNase HII and *Afu*RNase HII exhibit conserved secondary structure elements, with the exception that the  $\alpha$ 9-helix is incomplete in *Afu*RNase. This secondary structure element is important for *Tko*RNase HII to bind the substrate (19). Structural alignments resulted in the identification of conserved active site residues (Asp7, Glu8, Asp105 and Asp135) in *Pab*RNase HII, suggesting a similar catalytic mechanism between the three enzymes.

### Enzymatic properties of *P. abyssi* RNase HII

His-tagged *Pab*RNase HII was overproduced in *E. coli* and purified to give a single band on SDS-PAGE (Fig. 1B, lane 2). Reactions were carried out at 60 °C, the optimum temperature for *Pab*RNase HII activity (16). *Pab*RNase HII was assayed under different pH and ionic conditions, varying both the nature and the concentration of divalent cations, according to the general procedure described in Materials and methods using the RNA-DNA/DNA substrate (S1). The optimum pH for its activity was observed between pH 8.0 and 8.5 (Fig. 1C). However, at pH 7.5 and 9, the enzyme retained about 60 % of the activity measured at pH 8.

*Pab*RNase HII exhibited enzymatic activity in the presence of MgCl<sub>2</sub>, MnCl<sub>2</sub> and CoCl<sub>2</sub> (Fig. 1D). While *Pab*RNase HII activity was entirely dependent on the presence of a divalent cation, the enzyme was not active in the presence of NiCl<sub>2</sub>, FeCl<sub>2</sub>, ZnCl<sub>2</sub>, CaCl<sub>2</sub> or CuSO<sub>4</sub>. The most preferred metal ion for *Pab*RNase HII was MgCl<sub>2</sub> but the MnCl<sub>2</sub> and CoCl<sub>2</sub> could substitute for the MgCl<sub>2</sub> with reduced cleavage activity. As shown in Fig. 1D, the metal concentrations which gave the highest enzymatic activity were 5 mM for MgCl<sub>2</sub>, and 2 mM for MnCl<sub>2</sub> and CoCl<sub>2</sub>. Substrate hydrolysis in the presence of 5 mM for MgCl<sub>2</sub> was 1.5- and 3.2- fold higher than those determined at 2 mM for MnCl<sub>2</sub> and CoCl<sub>2</sub>, respectively. The kinetic parameters of *Pab*RNase HII were determined in the presence of RNA-DNA/DNA substrate (S1) and 5 mM MgCl<sub>2</sub>. The results are summarized in Table 2 and compared to that of type 2 RNase H archaeal homologue from *Archaeoglobus fulgidus* (*Afu*RNase HII) as already described (4). Interestingly, *Afu*RNase HII showed stronger substrate binding affinity than *Pab*RNase HII, as attested by a 10-fold lower  $K_m$  value, while the catalytic rate constants of the two enzymes were similar (Table 2). As a consequence, *Pab*RNase HII displayed a lower catalytic efficiency on RNA-DNA/DNA substrate as compared to *Afu*RNase HII (Table 2).

### **Ribonuclease activity of *P. abyssi* RNase HII**

Firstly, we examined whether *Pab*RNase HII could cleave the RNA strand of a RNA/DNA duplex (S11). As shown in Fig. 2, different 5'-terminal RNA products accumulated depending on the enzyme concentration, indicating that *Pab*RNase HII exhibited endoribonuclease activity. Because control assays without enzyme showed background degradation of the RNA primer (Fig. 2A, lane 2), they were subtracted from cleavage products signal. Less than 19 % intact RNA was present upon incubation with 100 nM *Pab*RNase HII for 30 min at 60°C (Fig.

2A, lane 6). Multiple cleavage sites were detected (Fig. 2A, lanes 2-8) and comparative analysis of products with those from the snake venom phosphodiesterase digest of 5'-end labelled 32 nucleotide (nt) RNA ladder (Fig. 2A, lane 1) pointed out main cleavage events (6-, 8-, 9-, 12-, 13- and 17-nt). Moreover, further processing of short RNA fragments could be observed by increasing enzyme concentrations. It is important to note that *PabRNase HII* used in this study did not exhibit nuclease activity on single-stranded RNA (Fig. 2B). All together, these results provided evidence that *PabRNase HII* acts as an endoribonuclease on RNA/DNA duplexes.

### **Structure-specific cleavage activities in *P. abyssi* RNase HII**

The absence of cleavage specificity of RNA/DNA duplexes prompted us to look for digestion of other relevant physiological substrates. We hypothesize that *PabRNase HII* participates in the mechanism of RNA primer removal, an activity which can occur once at the leading strand or much more frequently at the lagging strand. Therefore, we explored the cleavage specificity of *PabRNase HII* for substrates with Okazaki fragment-like intermediates.

#### *PabRNase HII specifically cleaves RNA-initiated DNA segments fully annealed to a DNA template*

We initially began to examine whether *PabRNase HII* could hydrolyse a cognate double-stranded Okazaki fragment (15). A single strand composed of 12 nucleotides of RNA (RNA12nt) followed by 18 nucleotides of DNA (DNA18nt), fluorescently labelled at the 5'-end, was annealed to a complementary 30 nucleotides DNA template to form the S1 substrate as shown in Fig. 3A. When this substrate was incubated in the presence of increasing *PabRNase HII* amounts, a major product appeared (Fig. 3B, lanes 2-5). This oligomer was

shown to correspond to 11 nucleotides RNA by migration with respect to a snake venom phosphodiesterase-generated digest of RNA12ntDNA18nt (Fig. 3B, lane 1). In addition to this main cleavage site, minor cleavage sites characteristic of non-specific nuclease activity were also found throughout the length of the RNA (Fig. 3B, lanes 2-5). Over time, *PabRNase HII* activity released the same oligomer which was basically free of any additional shorter fragments, suggesting that this product was not transiently formed and prevailed during the reaction (data not shown). Interestingly, *PabRNase HII* did not hydrolyse single-stranded RNA12ntDNA18nt (Fig. 3B, lanes 6-9) indicating that cleavage is dependent on the heteroduplex structure. It is of note that the pale band at ~9-nt present at relatively constant levels did not correspond to a specific cleavage product (Fig. 3B, lanes 2-9). Absence of specific cleavage was also observed with substrates lacking the complementary DNA template to either the RNA12nt or the DNA18nt sequence (data not shown). While a fully annealed RNA12ntDNA18nt/DNA is definitely required to detect cleavage specificity, *PabRNase HII* did not hydrolyse the complementary DNA template (Fig. 3B, lanes 10-13). Shorter bands were not due to cleavage activity since they were detectable in all lanes with equal intensities even in the absence of enzyme. These data demonstrated that *PabRNase HII* can act endonucleolytically on initiator RNA and displays a specific cleavage activity dependent on the heteroduplex structure.

*PabRNase HII specifically cleaves the fully annealed RNA strand of Okazaki fragment-gapped intermediates but not a 5'-RNA flap*

Both at the leading and lagging strands, sequential enzymatic steps are thought to be part of the RNA primer elimination mechanism in *P. abyssi*. As a consequence, diverse structural Okazaki fragment-like substrates would arise. Therefore, we examined whether structural intermediates (S4, S5 and S6) which can be captured during the process (outlined in Fig. 4A)

could direct the cleavage activity of *PabRNase HII*. On the 40-gapped S4 intermediate composed of an upstream DNA primer and a downstream RNA-DNA fragment fully annealed to the complementary DNA template, *PabRNase HII* specifically cleaved the RNA segment, releasing one ribonucleotide attached to the DNA segment (Fig. 4B, lanes 1-4). During the elongation step, the size of the gap would decrease to reach the next RNA initiator. By reconstitution of model transient substrates, we demonstrated that both the 20-nt gapped S5 intermediate (Fig. 4B, lanes 5-8) and a nicked intermediate (data not shown) were specifically cleaved. Collectively, cleavage efficiencies of the gapped and nicked Okazaki fragment intermediates were comparable to those of double-stranded RNA-DNA fragments (Fig. 3B, lanes 2-5). However, on a 5'-RNA flap which can result from strand displacement activity by *PabpolD* of the next Okazaki fragment (11), *PabRNase HII* did not significantly release oligomers (Fig. 4B, lanes 9-12). It is of note that a faint intensifying band at 8-nt (Fig. 4B, lanes 9-12) did not correspond to a specific cleavage product. These results clearly indicated that *PabRNase HII* is not involved in the cleavage of single-stranded RNA initiator despite the presence of surrounding DNA duplexes. These data are consistent with our observations from Fig. 3B that *PabRNase HII* exclusively cuts double-stranded RNA-DNA/DNA substrates. Importantly, we demonstrated that *PabRNase HII* cleaves the RNA initiator fully annealed to the complementary DNA template independently of the size of the gap. In addition, we provided evidence that a 5'-RNA flap is not an appropriate substrate for *PabRNase HII*, suggesting the requirement of additional enzymes to fully ensure the removal of Okazaki fragment intermediates at the lagging strand.

*PabRNase HII specifically cuts the RNA-DNA/DNA when the RNA is completely annealed to the DNA template*

274 The above results indicated that *PabRNase HII* specifically cleaves the RNA in an RNA-  
275 DNA/DNA duplex one ribonucleotide upstream of the RNA-DNA junction. Based on this  
276 observation, we attempted to gain further information about the structure-specific recognition  
277 of the RNA-DNA junction. We predicted that mismatches located either downstream or  
278 upstream of the site of cleavage would alter the structure of the junction and prevent  
279 *PabRNase HII* from recognising and cutting the substrate. Such substrates, which can be  
280 created during priming and DNA synthesis in eukaryotes (28, 31), could also be relevant in *P.*  
281 *abyssi* cells. In particular, the priming heterodimeric polymerase in *P. abyssi*, *Pabp46/41*  
282 complex, does not possess 3'-5' exonucleolytic activity and can consequently misincorporate  
283 nucleotides, creating mismatched base pairs at or near the RNA-DNA junction.

284 The complementary DNA template was designed to produce specific mismatches with the  
285 RNA12ntDNA18nt strand (Fig. 5A). When the mismatch was the deoxynucleotide  
286 downstream of the site of cleavage, *PabRNase HII* efficiently cleaved the S7 substrate and cut  
287 at one site into the RNA segment, leaving a monoribonucleotide attached to the DNA18nt  
288 strand (Fig. 5B, lanes 2-5). Cleavage efficiencies were still comparable to those of model  
289 Okazaki fragments described above. This result seems to point out that a deoxynucleotide  
290 mismatched Okazaki fragment does not affect recognition and specific cleavage by *PabRNase*  
291 *HII*. We next considered that ribonucleotide mismatches positioned downstream (Fig. 5A, S8  
292 substrate) or upstream (Fig. 5A, S9 substrate) of the cutting site would be crucial for directing  
293 the cleavage specificity of *PabRNase HII*. Interestingly, the presence of the ribonucleotide  
294 just downstream of the cutting site induced random endonucleolytic cleavage with  
295 predominant products (Fig. 5B, lanes 6-9 and Fig. 5C, S8 substrate) and the percent of  
296 hydrolysed products was equivalent to that of Okazaki fragment-like substrates. When the  
297 ribonucleotide mismatch was positioned upstream of the site of cleavage, random  
298 endonucleolytic activity was enhanced but cleavage efficiencies were lowered (Fig. 5B, lanes

10-13). Multiple cleavage sites due to the loss of specificity appeared (Fig. 5C, S9 substrate). Taken together these data showed for the first time that an archaeal RNase HII requires complete hybridization of the RNA segment to the DNA template in order to confer specific cleavage of RNA-DNA/DNA duplexes.

#### *PabRNase HII specifically cuts a single embedded ribonucleotide in a DNA duplex*

We anticipated that *PabRNase HII* nuclease could act on a single ribonucleotide embedded in DNA. A single ribonucleotide in a DNA duplex could arise via misincorporation of ribonucleotide during DNA synthesis or by ligation of the monoribonucleotide attached to the DNA after cleavage of Okazaki fragments by type 2 RNase H (26). To determine whether an embedded ribonucleotide in DNA (S10 substrate) is a hydrolysable substrate, endonuclease activity of *PabRNase HII* was carried out. Fig. 6B, lanes 8-11 demonstrated that *PabRNase HII* was able to recognise and to cleave endonucleolytically on the 5'-side of an embedded monoribonucleotide. Additional fragments, shorter than the released 11-nt, were faintly detectable. Basically, cleavage efficiencies of a single embedded ribonucleotide were similar to those of model Okazaki fragment S1 substrate (Fig. 6B, compare lanes 2-5 and lanes 8-11). Overall, we showed that *PabRNase HII* is active on single embedded ribonucleotides in a DNA duplex and releases a major product consisting of a single ribonucleotide on the 5'-end of the downstream DNA segment.



## DISCUSSION

Two types of RNase H, type 1 and type 2, have been identified in a multiplicity of archaeal genomes. While most archaeal microorganisms have only one type of RNase H, a few archaea such as *Sulfolobus tokodaii* and *Haloferax volcanii* possess both types of RNase H. Although the physiological significance of multiple *rnh* genes in single archaeal genomes is not well understood, RNases H are thought to be involved in important cellular processes (3, 10, 16, 23, 24). Interestingly, archaeal type 2 RNase H appears more universal because the encoding gene is distributed in almost all archaeal genomes. Sequence comparison within archaeal type 2 RNases H revealed a high degree of sequence similarity with conserved active site residues, suggesting that these enzymes may have common biochemical properties (3, 9). In this report, we demonstrated that *PabRNase HII*, type 2 RNase H from *P. abyssi*, is as an alkaline enzyme. This property seems to be a hallmark of type 2 thermostable RNases H (3, 9, 22). In addition, *PabRNase HII* appeared to prefer the  $Mg^{2+}$  ion for RNase activity rather than  $Mn^{2+}$  or  $Co^{2+}$ . Distinct metal dependencies have been described for *Archaeoglobus fulgidus* and *Thermococcus kodakaraensis KOD1* RNase HII with  $Mn^{2+}$ - or  $Co^{2+}$ -preference, respectively (3, 9). Metal ion usage by archaeal RNases HII may be a consequence of the environmental conditions they thrive. It may also dictate the substrate requirement for hydrolysis and confer a specialised function to the enzyme in the maintenance of genome integrity. Determination of kinetic parameters highlighted that the homologous archaeal enzymes, *AfuRNase HII* and *PabRNase HII*, showed distinct catalytic efficiencies for RNA-DNA/DNA substrates. These results mainly reflected differences in substrate binding affinity. In general, biochemical discrepancies observed between the three enzymes are possibly related to variations in secondary structure elements and physicochemical parameters (e.g., isoelectric point). Despite these subtle differences, archaeal RNase HII seem to possess conserved structural features

344 required to specifically recognise a comparable region of the substrates, and to produce  
345 similar products. Like other type 2 archaeal RNase H, *PabRNase HII* behaved as an efficient  
346 endoribonuclease on RNA/DNA duplexes, stalling at particular sites (3, 9). Moreover, most of  
347 the biochemical features of *PabRNase HII* overlapped those of the eukaryotic equivalent, type  
348 2 RNase H, described as a key enzyme in Okazaki fragment processing (17).

349 With diverse constructs representing replication-fork intermediates, *PabRNase HII* made  
350 structure-specific endonucleolytic cleavage in the RNA initiator, leaving a single  
351 ribonucleotide at the 5'-end of the RNA-DNA junction. Cleavage 5' to the junctional  
352 ribonucleotide required the presence of double-stranded substrates with the RNA segment  
353 fully annealed to the complementary strand. Gapped double-stranded substrates containing  
354 RNA-DNA junctions did not alter cleavage specificity. However, a single-stranded 5'-RNA  
355 flap was resistant to cleavage activity, indicating that *PabRNase HII* does not carry out this  
356 reaction at the replication fork. On the other hand, other results have demonstrated that the  
357 structure-specific nuclease, Flap endonuclease I (Fen I), can cleave substrates with RNA flap  
358 structures, bypassing the need for RNase HII in Okazaki fragment processing.(18, 27).

359 Furthermore, we demonstrated that mismatches in the RNA portion, produced by erroneous  
360 priming and polymerising activities during initiation of DNA replication in eukaryotes (28,  
361 31), resulted in loss of specificity by *PabRNase HII*. These results demonstrate, for the first  
362 time, that the RNA residues in the vicinity of the RNA-DNA junction are key structural  
363 determinants for cleavage specificity of type 2 archaeal RNase H. Notably, archaeal type 2  
364 RNase H seems to differ from eukaryotic type 2 (17) in that it recognizes the RNA strand  
365 rather than the RNA-DNA junction. Possibly, the RNA portion of the RNA-DNA junction  
366 annealed to DNA template adopts an intermediate helical structure, which might target RNase  
367 HII recognition and induce specific cleavage. This hypothesis is sustained by the observation  
368 that RNA/DNA and DNA/DNA duplexes form A-type and B-type helices, respectively (5, 7).

369 We recently proposed a model of DNA replication in *P. abyssi* that involves the family B  
370 DNA polymerase, *PabpolB*, at the leading strand and the family D DNA polymerase,  
371 *PabpolD*, at the lagging strand (11). This model is reinforced by complementary studies  
372 demonstrating that *PabpolB* is likely the leading strand DNA polymerase (25). Typically,  
373 *PabpolD* has the capacity to displace the downstream fragment including the RNA initiator,  
374 while *PabpolB* is not active on this substrate. In this situation, RNA-initiated DNA segments  
375 fully annealed to a DNA template would arise only at the leading strand. Because *PabRNase*  
376 HII cannot cleave 5'-RNA flap templates, *PabRNase* HII would recognize the annealed RNA  
377 primer at the leading strand and promotes its endonucleolytic cleavage. The resulting 5'  
378 phosphorylated junction ribonucleotide attached to the DNA would be subsequently displaced  
379 by *PabpolB* and cleaved by *PabFen* I, prior to ligation by *PabDNA* ligase I. Thus, the  
380 functional importance of RNase HII in the completion of leading strand DNA replication in *P.*  
381 *abyssi* awaits the *in vitro* reconstitution of this multi-step enzymatic process (manuscript in  
382 preparation). Despite common biochemical properties with the eukaryotic type 2 RNase H,  
383 single archaeal RNases HII could be cellular enzymes involved in the removal of RNA  
384 residues at the leading strand rather than at the lagging strand. Such biological assumptions  
385 would indicate that these microorganisms have evolved differently by targeting analogous  
386 enzymes to unrelated biological functions.

387 Moreover, we demonstrated that *PabRNase* HII is able to cleave at the 5'-end of single  
388 embedded ribonucleotides with similar efficiency as at cognate Okazaki fragments (15). Since  
389 such structural substrates can appear *in vivo* during Okazaki fragment processing from  
390 intrinsic RNA ligation activity or erroneous nucleotide incorporation (26) and during  
391 exposure to external damaging agents (32), we suggest that *PabRNase* HII can participate in  
392 the removal of inappropriate ribonucleotides from the hyperthermophilic chromosome. These  
393 biochemical characteristics would imply that *PabRNase* HII promotes the initial step of the

394 repair process as already observed in eukaryotes (26). However, reconstitution of the  
395 complete enzymatic process awaits further assessment.

396    **ACKNOWLEDGEMENTS**

397    We are grateful to Hannu Myllykallio for providing the expression clone encoding *PabRNase*  
398    HII and critical reading of the manuscript. This work was financially supported by the French  
399    institute of marine research and exploitation (Ifremer). Sébastien Le Laz thanks the University  
400    of Western Brittany for funding.

## REFERENCES

1. **Cann, I. K., K. Komori, H. Toh, S. Kanai, and Y. Ishino.** 1998. A heterodimeric DNA polymerase: evidence that members of Euryarchaeota possess a distinct DNA polymerase. *Proc Natl Acad Sci U S A* **95**:14250-5.
2. **Cerritelli, S. M., and R. J. Crouch.** 2009. Ribonuclease H: the enzymes in eukaryotes. *Febs J* **276**:1494-505.
3. **Chai, Q., J. Qiu, B. R. Chapados, and B. Shen.** 2001. *Archaeoglobus fulgidus* RNase HII in DNA replication: enzymological functions and activity regulation via metal cofactors. *Biochem Biophys Res Commun* **286**:1073-81.
4. **Chapados, B. R., Q. Chai, D. J. Hosfield, J. Qiu, B. Shen, and J. A. Tainer.** 2001. Structural biochemistry of a type 2 RNase H: RNA primer recognition and removal during DNA replication. *J Mol Biol* **307**:541-56.
5. **Chou, S. H., P. Flynn, and B. Reid.** 1989. Solid-phase synthesis and high-resolution NMR studies of two synthetic double-helical RNA dodecamers: r(CGCGAAUUCGCG) and r(CGCGUAUACGCG). *Biochemistry* **28**:2422-35.
6. **Cohen, G. N., V. Barbe, D. Flament, M. Galperin, R. Heilig, O. Lecompte, O. Poch, D. Prieur, J. Querellou, R. Ripp, J. C. Thierry, J. Van der Oost, J. Weissenbach, Y. Zivanovic, and P. Forterre.** 2003. An integrated analysis of the genome of the hyperthermophilic archaeon *Pyrococcus abyssi*. *Mol Microbiol* **47**:1495-512.
7. **Dickerson, R. E., H. R. Drew, B. N. Conner, R. M. Wing, A. V. Fratini, and M. L. Kopka.** 1982. The anatomy of A-, B-, and Z-DNA. *Science* **216**:475-85.
8. **Gueguen, Y., J. L. Rolland, O. Lecompte, P. Azam, G. Le Romancer, D. Flament, J. P. Raffin, and J. Dietrich.** 2001. Characterization of two DNA polymerases from the hyperthermophilic euryarchaeon *Pyrococcus abyssi*. *Eur J Biochem* **268**:5961-9.

- 427 9. **Haruki, M., K. Hayashi, T. Kochi, A. Muroya, Y. Koga, M. Morikawa, T.**  
428 **Imanaka, and S. Kanaya.** 1998. Gene cloning and characterization of recombinant  
429 RNase HII from a hyperthermophilic archaeon. *J Bacteriol* **180**:6207-14.
- 430 10. **Haruki, M., Y. Tsunaka, M. Morikawa, and S. Kanaya.** 2002. Cleavage of a DNA-  
431 RNA-DNA/DNA chimeric substrate containing a single ribonucleotide at the DNA-  
432 RNA junction with prokaryotic RNases HII. *FEBS Lett* **531**:204-8.
- 433 11. **Henneke, G., D. Flament, U. Hubscher, J. Querellou, and J. P. Raffin.** 2005. The  
434 hyperthermophilic euryarchaeota *Pyrococcus abyssi* likely requires the two DNA  
435 polymerases D and B for DNA replication. *J Mol Biol* **350**:53-64.
- 436 12. **Lai, L., H. Yokota, L. W. Hung, R. Kim, and S. H. Kim.** 2000. Crystal structure of  
437 archaeal RNase HII: a homologue of human major RNase H. *Structure* **8**:897-904.
- 438 13. **Lao-Sirieix, S. H., and S. D. Bell.** 2004. The heterodimeric primase of the  
439 hyperthermophilic archaeon *Sulfolobus solfataricus* possesses DNA and RNA  
440 primase, polymerase and 3'-terminal nucleotidyl transferase activities. *J Mol Biol*  
441 **344**:1251-63.
- 442 14. **Le Breton, M., G. Henneke, C. Norais, D. Flament, H. Myllykallio, J. Querellou,**  
443 **and J. P. Raffin.** 2007. The heterodimeric primase from the euryarchaeon *Pyrococcus*  
444 *abyssi*: a multifunctional enzyme for initiation and repair? *J Mol Biol* **374**:1172-85.
- 445 15. **Matsunaga, F., C. Norais, P. Forterre, and H. Myllykallio.** 2003. Identification of  
446 short 'eukaryotic' Okazaki fragments synthesized from a prokaryotic replication origin.  
447 *EMBO Rep* **4**:154-8.
- 448 16. **Meslet-Cladiere, L., C. Norais, J. Kuhn, J. Briffotiaux, J. W. Sloostra, E. Ferrari,**  
449 **U. Hubscher, D. Flament, and H. Myllykallio.** 2007. A novel proteomic approach  
450 identifies new interaction partners for proliferating cell nuclear antigen. *J Mol Biol*  
451 **372**:1137-48.

- 452 17. **Murante, R. S., L. A. Henricksen, and R. A. Bambara.** 1998. Junction  
453 ribonuclease: an activity in Okazaki fragment processing. *Proc Natl Acad Sci U S A*  
454 **95**:2244-9.
- 455 18. **Murante, R. S., J. A. Rumbaugh, C. J. Barnes, J. R. Norton, and R. A. Bambara.**  
456 1996. Calf RTH-1 nuclease can remove the initiator RNAs of Okazaki fragments by  
457 endonuclease activity. *J Biol Chem* **271**:25888-97.
- 458 19. **Muroya, A., D. Tsuchiya, M. Ishikawa, M. Haruki, M. Morikawa, S. Kanaya,**  
459 **and K. Morikawa.** 2001. Catalytic center of an archaeal type 2 ribonuclease H as  
460 revealed by X-ray crystallographic and mutational analyses. *Protein Sci* **10**:707-14.
- 461 20. **Nick McElhinny, S. A., B. E. Watts, D. Kumar, D. L. Watt, E. B. Lundstrom, P.**  
462 **M. Burgers, E. Johansson, A. Chabes, and T. A. Kunkel.** 2010. Abundant  
463 ribonucleotide incorporation into DNA by yeast replicative polymerases. *Proc Natl*  
464 *Acad Sci U S A* **107**:4949-54.
- 465 21. **Ohtani, N., M. Haruki, M. Morikawa, and S. Kanaya.** 1999. Molecular diversities  
466 of RNases H. *J Biosci Bioeng* **88**:12-9.
- 467 22. **Ohtani, N., M. Tomita, and M. Itaya.** 2008. Junction ribonuclease: a ribonuclease  
468 HII orthologue from *Thermus thermophilus* HB8 prefers the RNA-DNA junction to  
469 the RNA/DNA heteroduplex. *Biochem J* **412**:517-26.
- 470 23. **Ohtani, N., H. Yanagawa, M. Tomita, and M. Itaya.** 2004. Cleavage of double-  
471 stranded RNA by RNase HI from a thermoacidophilic archaeon, *Sulfolobus tokodaii* 7.  
472 *Nucleic Acids Res* **32**:5809-19.
- 473 24. **Ohtani, N., H. Yanagawa, M. Tomita, and M. Itaya.** 2004. Identification of the first  
474 archaeal Type 1 RNase H gene from *Halobacterium* sp. NRC-1: archaeal RNase HI  
475 can cleave an RNA-DNA junction. *Biochem J* **381**:795-802.



- 476 25. **Rouillon, C., G. Henneke, D. Flament, J. Querellou, and J. P. Raffin.** 2007. DNA  
477 polymerase switching on homotrimeric PCNA at the replication fork of the  
478 euryarchaea *Pyrococcus abyssi*. J Mol Biol **369**:343-55.
- 479 26. **Rumbaugh, J. A., R. S. Murante, S. Shi, and R. A. Bambara.** 1997. Creation and  
480 removal of embedded ribonucleotides in chromosomal DNA during mammalian  
481 Okazaki fragment processing. J Biol Chem **272**:22591-9.
- 482 27. **Sato, A., A. Kanai, M. Itaya, and M. Tomita.** 2003. Cooperative regulation for  
483 Okazaki fragment processing by RNase HII and FEN-1 purified from a  
484 hyperthermophilic archaeon, *Pyrococcus furiosus*. Biochem Biophys Res Commun  
485 **309**:247-52.
- 486 28. **Sheaff, R. J., and R. D. Kuchta.** 1994. Misincorporation of nucleotides by calf  
487 thymus DNA primase and elongation of primers containing multiple noncognate  
488 nucleotides by DNA polymerase alpha. J Biol Chem **269**:19225-31.
- 489 29. **Stein, H., and P. Hausen.** 1969. Enzyme from calf thymus degrading the RNA  
490 moiety of DNA-RNA Hybrids: effect on DNA-dependent RNA polymerase. Science  
491 **166**:393-5.
- 492 30. **Tadokoro, T., and S. Kanaya.** 2009. Ribonuclease H: molecular diversities, substrate  
493 binding domains, and catalytic mechanism of the prokaryotic enzymes. Febs J  
494 **276**:1482-93.
- 495 31. **Thomas, D. C., J. D. Roberts, R. D. Sabatino, T. W. Myers, C. K. Tan, K. M.**  
496 **Downey, A. G. So, R. A. Bambara, and T. A. Kunkel.** 1991. Fidelity of mammalian  
497 DNA replication and replicative DNA polymerases. Biochemistry **30**:11751-9.
- 498 32. **Von Sonntag, C., and D. Schulte-Frohlinde.** 1978. Radiation-induced degradation of  
499 the sugar in model compounds and in DNA. Mol Biol Biochem Biophys **27**:204-26.

## FIGURE LEGENDS

**Fig. 1 Enzymatic properties of *Pab*RNase HII.** (A) Alignment of the amino acid sequences of archaeal RNase HII homologues. Sequences are from the three euryarchaeota species, *P. abyssi* (Pab, accession number, gi: 14520734), *T. kodakaraensis KOD1* (Tko, accession number, gi: 57640740), *A. fulgidus* (Afu, accession number, gi: 11498229). Conserved amino acid residues are shaded black. Similar amino acid residues are framed black. Proposed active sites residues are indicated by asterisks. Secondary structure is shown above the sequences, denoting  $\beta$ -sheets (arrows) and  $\alpha$ -helices (ribbons). (B) SDS-PAGE gradient gel (4-20 %) of purified, recombinant His<sub>6</sub>-tagged *Pab*RNase HII (0.5  $\mu$ g; lane 2) and molecular mass markers (lane 1) stained with Coomassie Blue (C) pH dependence. The enzymatic activities were determined at 60°C for 30 min in reaction buffer containing 50 mM Tris-HCl, 5 mM dithiothreitol, 5 mM MgCl<sub>2</sub>, 50 nM of *Pab*RNase HII and 50 nM of RNA-DNA/DNA substrate (S1) with pH values ranging from 5 to 10. Data are the average of triplicate measurements. (D) Divalent cation dependence. The enzymatic activities were determined at 60°C for 30 min in reaction buffer containing 50 mM Tris-HCl (pH 8), 5 mM dithiothreitol, 50 nM of *Pab*RNase HII and 50 nM of RNA-DNA/DNA substrate (S1) at the indicated concentrations of MgCl<sub>2</sub> (◆), MnCl<sub>2</sub> (Δ) and CoCl<sub>2</sub> (■). Data are the average of triplicate measurements.

**Fig. 2 Ribonuclease activity by *Pab*RNase HII.** (A) Indicated amounts of *Pab*RNase HII were incubated with the S11 substrate (lanes 2-8) and a base-hydrolysed ladder (lane 1) was prepared as described (see Materials and methods section). 5'-end fluorescently labelled products were visualised with a Mode Imager Typhoon 9400 (GE Healthcare) and quantification was performed using Image Quant 5.2 software. (B) *Pab*RNase HII was

incubated with the 32-base single-stranded RNA oligonucleotide at the indicated amounts (lanes 1-4). An 8-nt RNA oligonucleotide was used as a ladder (lane 5). 5'-end fluorescently labelled products were visualised with a Mode Imager Typhoon 9400 (GE Healthcare).

**Fig. 3 *PabRNaseHII* specifically cleaves RNA-initiated DNA segments fully annealed to a DNA template.** (A) Substrate structure representations of S1, S2, and S3. The thick line and the closed circle represent the RNA portion and the fluorescent label, respectively. (B) Indicated amounts of *PabRNase HII* were incubated with S1 substrate (lanes 2-5), S2 substrate (lanes 6-9) and S3 substrate (lanes 10-13). A base-hydrolysed ladder (lane 1) was prepared as explained in the Materials and methods section. Fluorescent-labelled products were visualised with a Mode Imager Typhoon 9400 (GE Healthcare) and quantification was performed using Image Quant 5.2 software.

**Fig. 4 *PabRNase HII* specifically cleaves the fully annealed RNA strand of Okazaki fragment-gapped intermediates but not a 5'-RNA flap.** (A) Substrate structure representations of S4, S5, and S6. The thick line and the closed circle represent the RNA portion and the fluorescent label, respectively. (B) Indicated amounts of *PabRNase HII* were incubated with S4 substrate (lanes 1-4), S5 substrate (lanes 5-8) and S6 substrate (lanes 9-12). An 18-nt nucleotide was used as an appropriate ladder (lane 13). Fluorescent-labelled products were visualised with a Mode Imager Typhoon 9400 (GE Healthcare) and quantification was performed using Image Quant 5.2 software.

**Fig. 5 *PabRNase HII* specifically cuts the RNA-DNA/DNA when the RNA is completely annealed to the DNA template.** (A) Substrate structure representations of S7, S8, and S9. The thick line and the closed circle represent the RNA portion and the fluorescent label,

respectively. (B) Indicated amounts of *PabRNase HII* were incubated with S7 substrate (lanes 2-5), S8 substrate (lanes 6-9) and S9 substrate (lanes 10-13). An 11-nt nucleotide was used as an appropriate ladder (lane 1). Fluorescent-labelled products were visualised with a Mode Imager Typhoon 9400 (GE Healthcare) and quantification was performed using Image Quant 5.2 software. (C) Graphical representation of sites and extents of cleavage in mismatches RNA-DNA/DNA substrates. Cleavage sites are denoted by different bars. Deoxyribonucleotides and ribonucleotides are shown by uppercase and lowercase letters, respectively.

**Fig. 6 *PabRNase HII* specifically cuts single embedded ribonucleotide in a DNA duplex.**

(A) Substrate structure representations of S1 and S10. The thick line and the closed circle represent the RNA portion and the fluorescent label, respectively. (B) Indicated amounts of *PabRNase HII* were incubated with S1 substrate (lanes 2-5) and S10 substrate (lanes 8-11). Both substrates and the corresponding hydrolysed products were manually labelled. Lanes 1 and 6 are appropriate 11-nt and 12-nt ladders for hydrolysed S1 substrates. Lanes 7 and 12 are suitable 11-nt and 12-nt ladders for hydrolysed S10 substrates. Fluorescent-labelled products were visualised with a Mode Imager Typhoon 9400 (GE Healthcare) and quantification was performed using Image Quant 5.2 software.

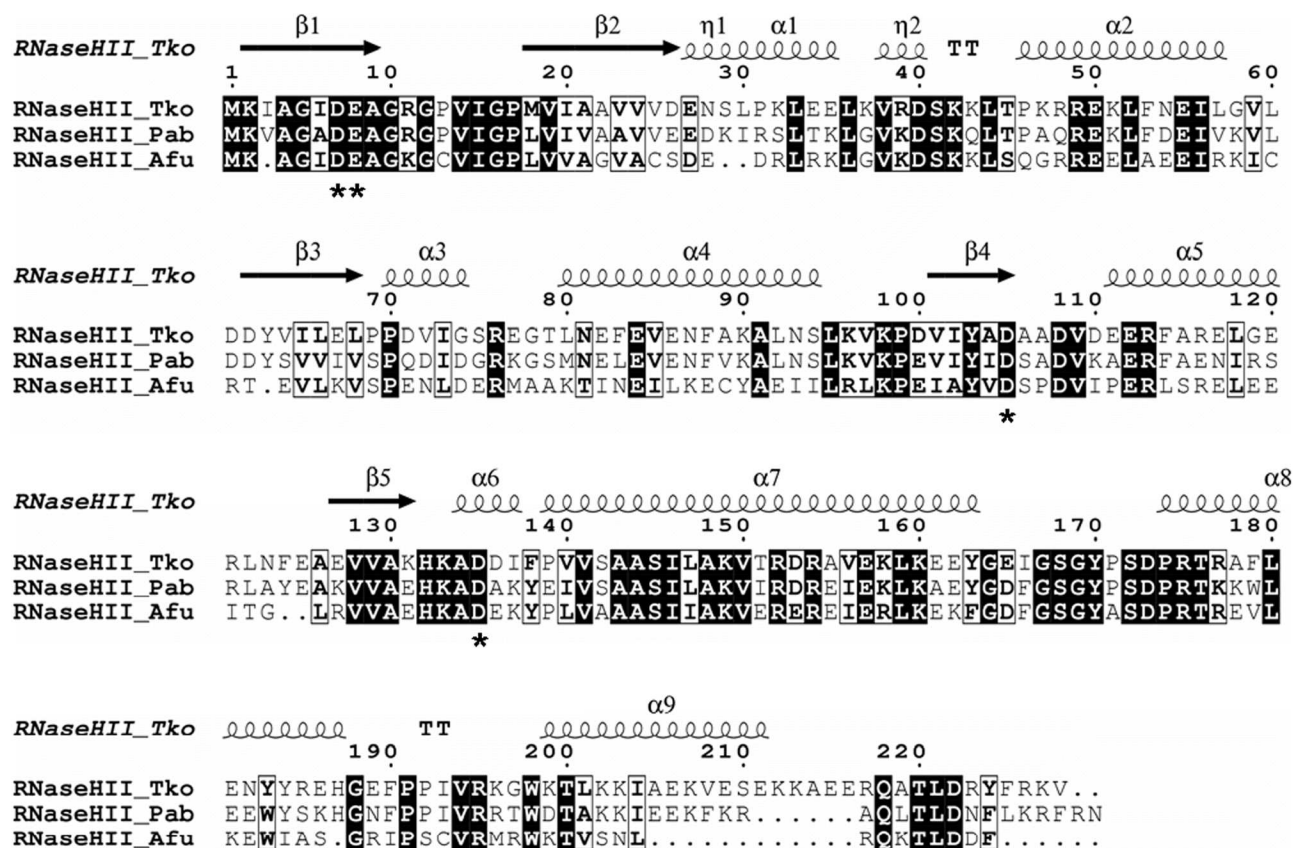
**TABLE 1 Oligonucleotide sequences used to create structural duplex substrates**

S1 substrate comprises primers 2 and template 8; S2 substrate is primer 2; S3 substrate comprises primers 2 and template 8; S4 substrate consists of primers 2, 3 and template 7; S5 substrate contains primers 2, 4 and template 7; S6 substrate includes primers 2, 5 and template 9; S7 substrate consists of primer 2 and template 12; S8 substrate is composed of primer 2 and template 11; S9 substrate consists of primer 2 and template 10; S10 substrate comprises

primer 6 and template 8; S11 substrate contains primer 1 and template 7. Deoxyribonucleotides and ribonucleotides are shown by uppercase and lowercase letters, respectively.

**TABLE 2     Kinetic parameters of archaeal RNase HII.** Hydrolyses of RNA-DNA/DNA substrates (S1) were carried out at 60°C in *PabRNase HII* reaction buffer as described in the Materials and methods section. The data were fit by nonlinear regression using the Marquardt-Levenberg algorithm (EnzFitter 2.0, BioSoft) to the Michaelis-Menten equation. Kinetic parameters,  $K_m$  and  $V_{max}$ , obtained from the fit were used to calculate the catalytic efficiency ( $k_{cat}/K_m$ ) of *PabRNase HII*. The kinetics values are the average of at least triplicate determinations and are shown with standard deviations (SD). Kinetic parameters of *AfuRNase HII* were extracted from previous studies (4).

A



B

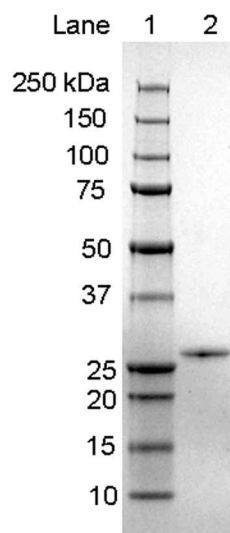


Fig. 1

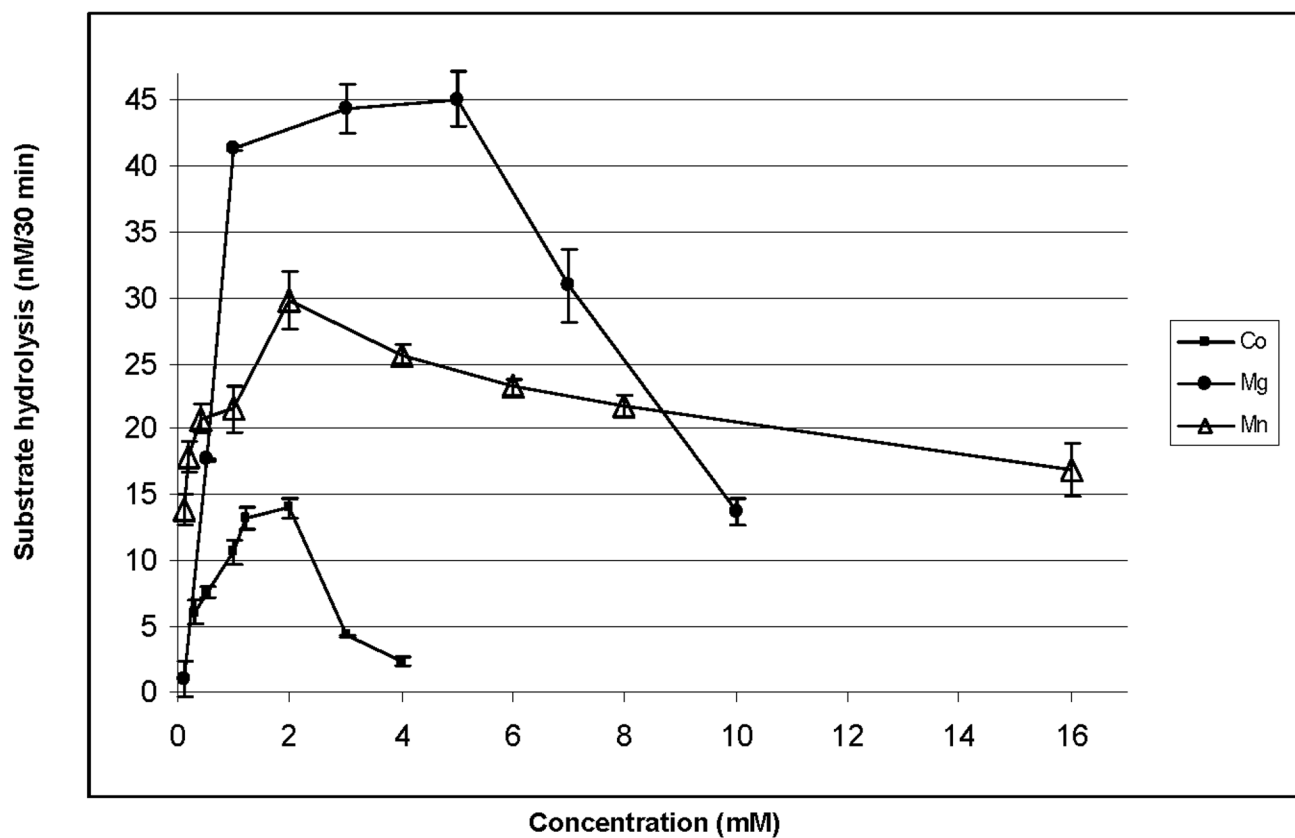
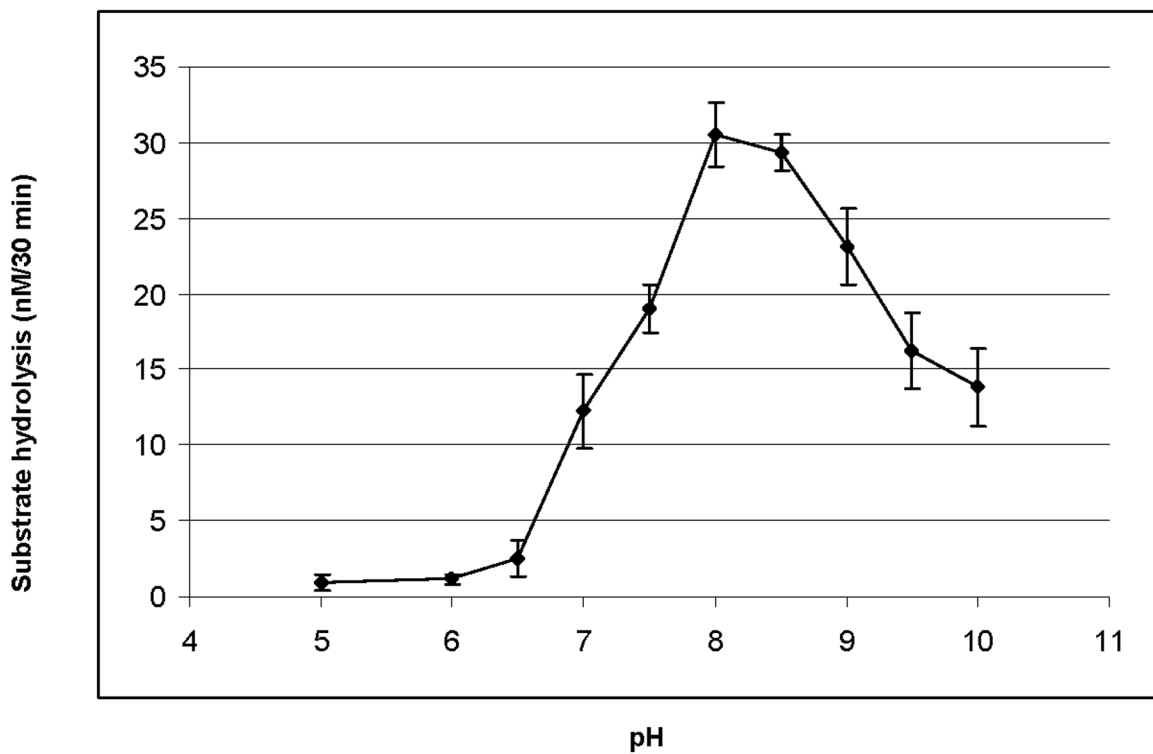
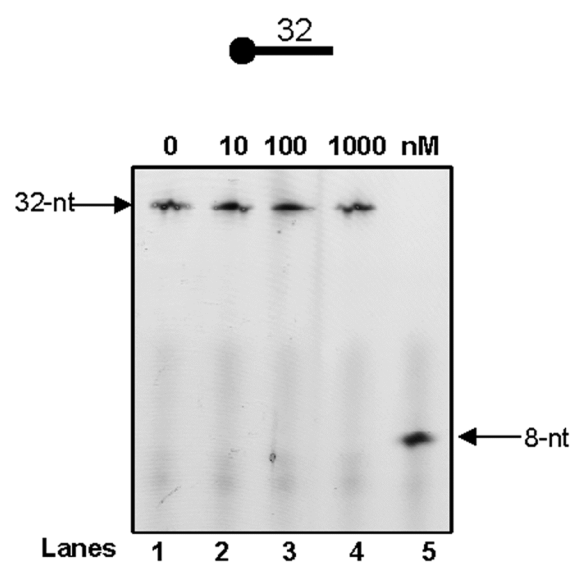
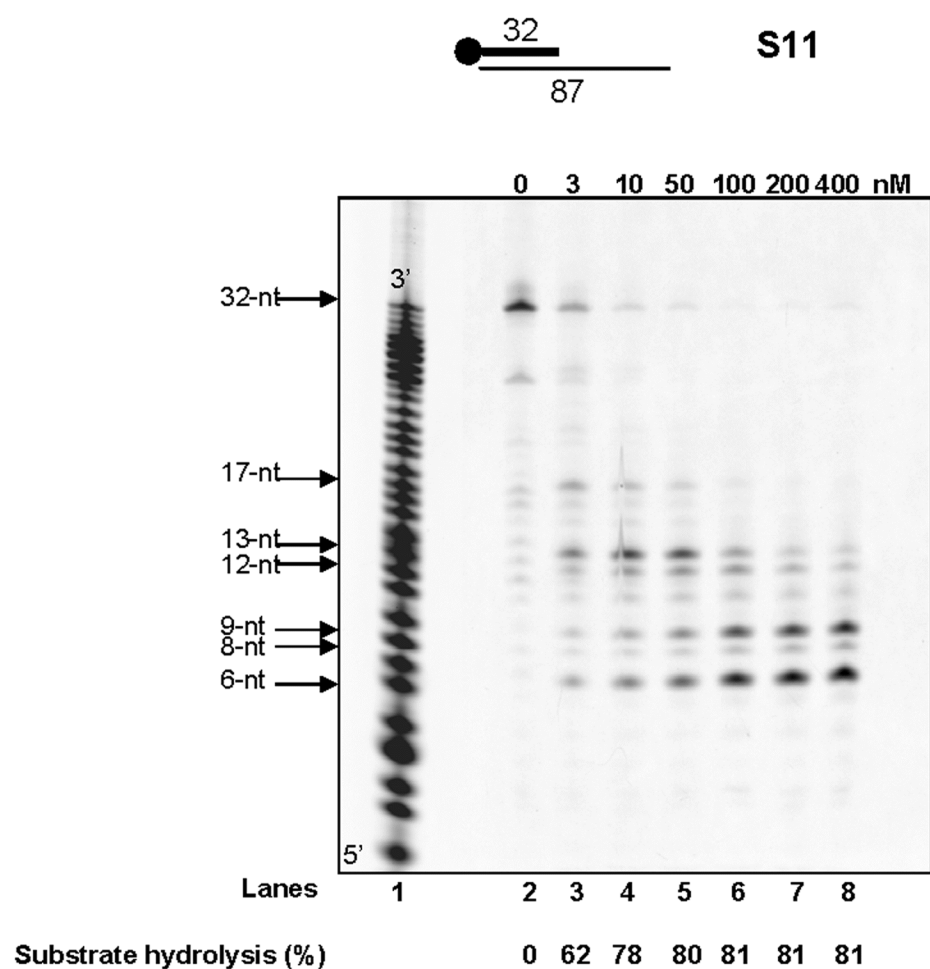
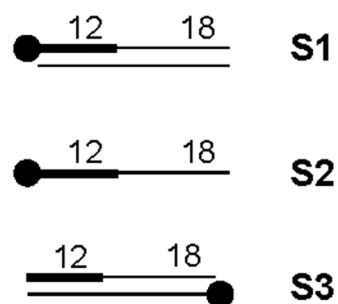


Fig. 1

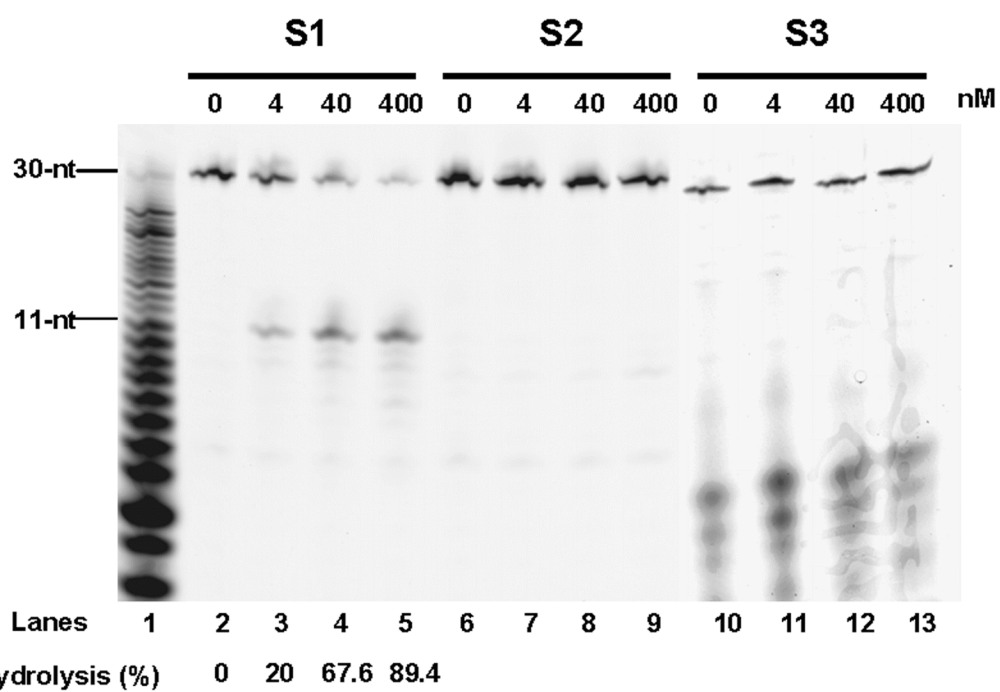


**Fig. 2**



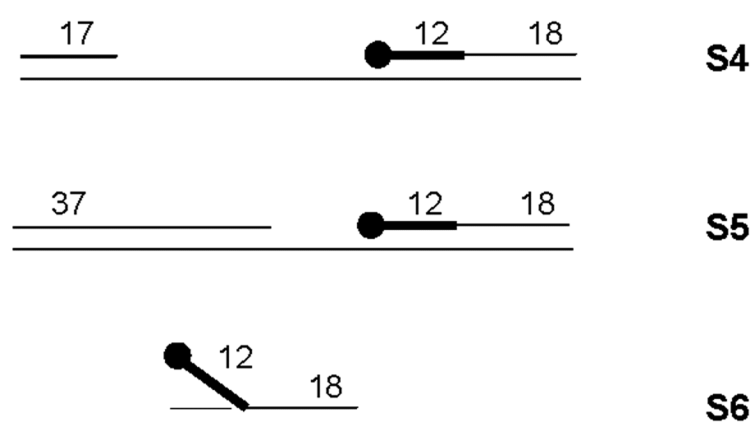


**A**

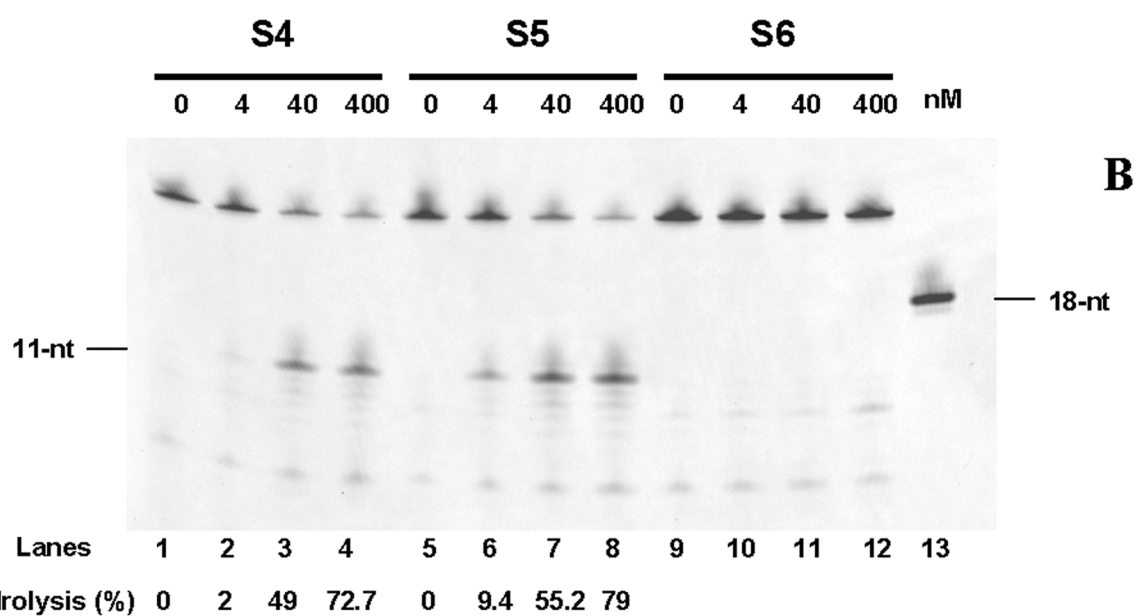


**B**

**Fig. 3**

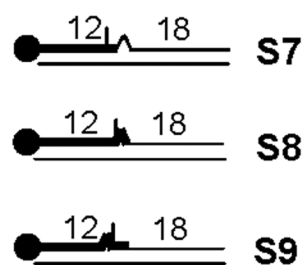


**A**

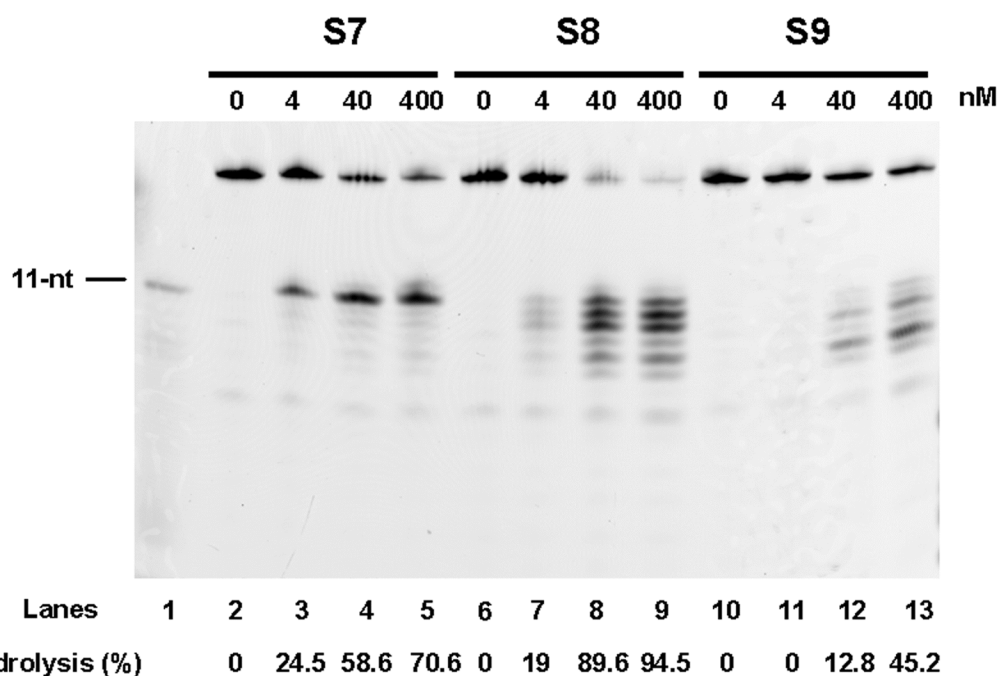


**B**

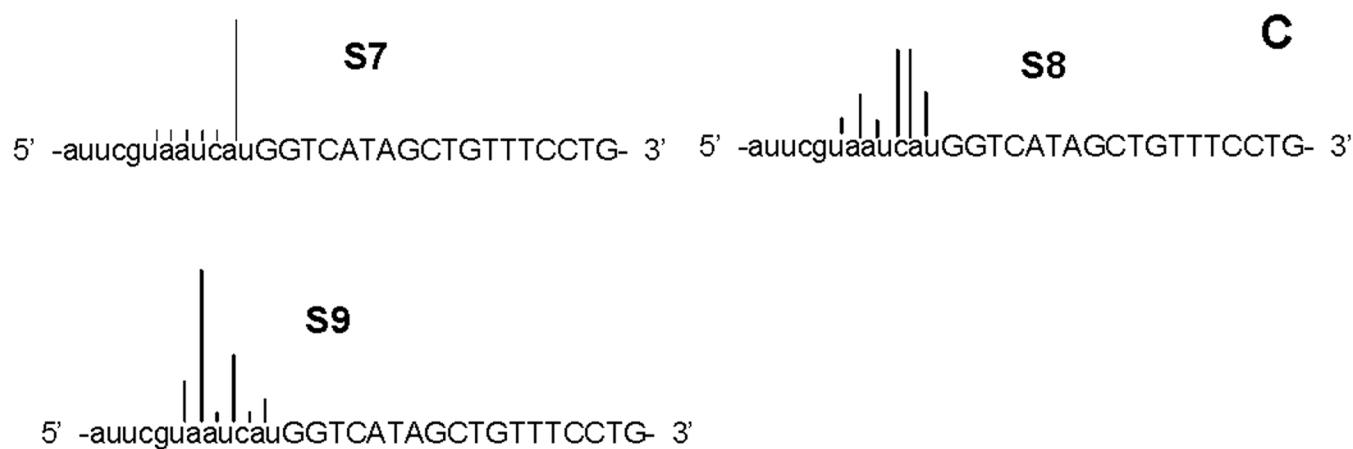
**Fig. 4**



**A**



**B**



**C**

**Fig. 5**



**A**

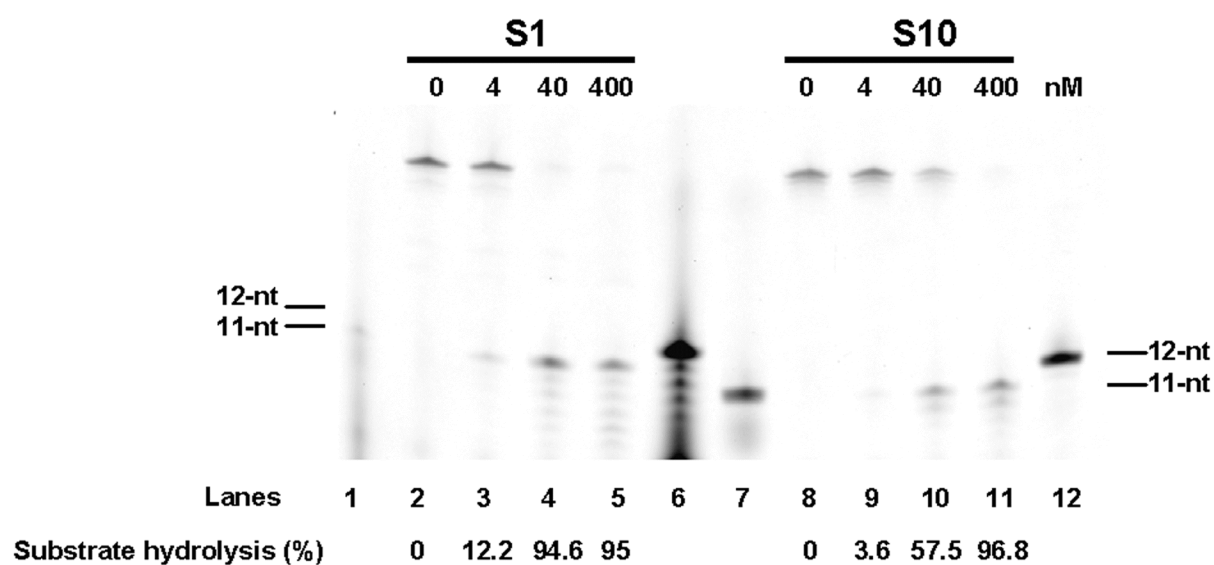


**Fig. 6**

<b>Primers</b>	<b>Length</b>	<b>Sequence</b>
1	32-nt	ugccaagcuugcaugccugcaggucgacucua
2	30-nt	auucguaaucauGGTCATAGCTGTTTCCTG
3	17-nt	TGCCAAGCTTG CATGCC
4	37-nt	TGCCAAGCTTG CATGCCTGCAGGTCGACTCTAGAGGA
5	12-nt	TGGGTGGGGTGG
6	30-nt	ATTCGTAATCAuGGTCATAGCTGTTTCCTG
<b>Templates</b>	<b>Length</b>	<b>Sequence</b>
7	87-nt	CAGGAAACAGCTATGACCATGATTACGAATTCGAGCTCGGTACCCGGGGATCCTCTAGAGTCGACCTGCAGGCATG CAAGCTTGGCA
8	30-nt	CAGGAAACAGCTATGACCATGATTACGAAT
9	30-nt	CAGGAAACAGCTATGACCCACCCACCCA
10	30-nt	CAGGAAACAGCTATGACCAGGATTACGAAT
11	30-nt	CAGGAAACAGCTATGACCGTGATTACGAAT
12	30-nt	CAGGAAACAGCTATGACTATGATTACGAAT

Table1

Enzymes	$K_m$ ( $\mu\text{M}$ )	$k_{cat}$ ( $\text{min}^{-1}$ )	$k_{cat}/K_m$
<i>Pab</i> RNase HII	0.50 $\pm$ 0.15	5.57 $\pm$ 0.54	11.14
<i>Afu</i> RNase HII	0.06 $\pm$ 0.15	8.0 $\pm$ 0.23	133.3

**Table 2**